Arabian Journal for Science and Engineering
https://doi.org/10.1007/s13369-020-04952-2

RESEARCH ARTICLE-CHEMISTRY

Fabrication and Characterization of UHMWPE–Ni Composites for Enhanced Electromagnetic Interference Shielding

G. Celebi Efe[1,2] · I. Altinsoy[3] · S. Ç. Yener[4,5] · T. Yener[3] · M. Ipek[3] · C. Bindal[2,3] · A. H. Ucisik[6]

Received: 30 January 2020 / Accepted: 17 September 2020

Abstract

Nickel-plated ultrahigh molecular weight polyethylene (UHMWPE) samples were prepared by an electroless coating method followed by hot pressing. The concentration of Ni in the composites was varied between 3.98 and 10.88 in volume percentage. XRD results revealed that Ni coating was successfully realized on the surface of UHWMPE particles confirmed by SEM–EDS. Ni thickness on the UHMWPE particles has thickness of 2 µm and there was also self-precipitated Ni plates as well as additive Ni particles according to SEM. Hardness values of Ni-coated UHMWPE–Ni composites increased 30% with increasing Ni content. The EMI-SE of the composite increased from 49 up to 70 dB by increasing Ni content for both X and Ku-band with respect to Ni concentration. Our samples, performed very high shielding within X band and also Ku band compared to most of other reports in the open literature, can be suitable for high-performance requirements especially in aerospace applications.

Keywords UHWWPE · Electroless plating · EMI shielding · Polymer composites · EMI SE

1 Introduction

Today, we live in an environment surrounded by electromagnetic radiation of various frequencies (10^4–10^{12} Hz), which we cannot realize with our senses [1, 2]. Electromagnetic radiation or EMI in a nutshell, refers to the energy convoy emitted from any source by the speed of light in all directions. In industrial and domestic environments; such as personal computer, servers, relays, DC electric motors, welding units and fluorescent lights, etc., switched devices form electromagnetic waves rich in spectral content [1, 3].

Therefore, the problem of electromagnetic radiation protection has a very important technical direction in relation to a reduction in the electromagnetic interference level (EMI) occurring between electronic devices [4]. With every passing day, EMI shielding materials draw more attention to protect the working area and the environment from electromagnetic radiation from electronic devices [5].

Electromagnetic shielding is defined to encapsulate electromagnetic energy within a certain defined area and/or to prevent this energy from spreading to a designated area [4]. All of the main purpose of all shielding materials and products used for this consecept are related to the conductivity of the metal elements they contain. As very well known all conductive materials reflect electromagnetic waves/EMFs due to the presence of free electrons in their mass. The higher the conductivity, the greater the EMF/wave shot and the projection. So it can be said that the best conductive materials are metals. All metallic surfaces have a reflective effect on electromagnetic waves due to their free electrons [6].

Metals and metal alloys are the best EMI shielding materials due to their excellent electrical conductivity. However, metals generally do not have the ductility and flexibility required for extensive deformations encountered in consumer devices. Metals are heavy, exposed to corrosion and

✉ T. Yener
tcerezci@sakarya.edu.tr

1 Department of Metallurgy and Materials Engineering, Faculty of Technology, Sakarya University of Applied Sciences, 54187 Sakarya, Turkey

2 Biomedical, Magnetic and Semi Conductive Materials Research Center (BIMAS-RC), Sakarya University, Esentepe Campus, 54187 Sakarya, Turkey

3 Department of Metallurgy and Materials Engineering, Engineering Faculty, Sakarya University, Esentepe Campus, 54187 Sakarya, Turkey

4 Department of Electrical and Electronic Engineering, Engineering Faculty, Sakarya University, Esentepe Campus, 54187 Sakarya, Turkey

5 Electromagnetics Research Center, Sakarya University, Esentepe Campus, 54187 Sakarya, Turkey

6 Turkish Aerospace Industry, 06980 Ankara, Turkey

Published online: 09 October 2020

often require very detailed and long production procedures that further limit their use in today's EMI applications. For this reason, there is an urgent need for functional materials with ultra-thin, lightweight, highly flexible and corrosion-resistant EMI shielding [7, 8]. In recent years, conductive polymer composites (CPC) have attracted a great deal of attention with its very common usage [9] and replacing the already used high-density wearable metallic EMI shielding materials, lightweight, easy-handling capability and performances can be the best candidate for the current EMI shielding class environment. To address these issues, Ni-coated ultra-high-molecular weight polyethylene can be used an alternative material. Electroless plating is a method for the deposition of metals such as nickel and copper onto an insulating substrate via catalyzed chemical reduction in solution-phase metal ions at the substrate surface. In the field of electromagnetic shielding effective materials, nickel-coated polymer particles have been identified as an effective additive [10].

Smirnova et al. [11] mentioned in their paper importance of protection electronic devices in a board subjected to high-frequency electromagnetic emission is a crucial problem in terms of space flight safety. Current study focused on this important point and it was under debated electroless Ni-coated UHMWPE material as an candidate conductive polymeric material with in a high-electromagnetic shielding effect according to nickel amount within the coating on the UHMWPE for EMI-SE effectivity of the composites.

2 Experimental Study

UHMWPE powders (Sigma Aldrich, ~ 100 µm particle size) were used as substrate for electroless Ni plating process realized to develop highly conductive polymer composites for effective electromagnetic shielding. Prior to electroless Ni coating, UHMWPE powders were rinsed to $SnCl_2$ (99.9%, Sigma Aldrich) solution to sensitize surface and following by immersing into $PdCl_2$ (99.9% Alfa-Aesar) solution for 15 min to ensure-activated sites on the surface of polymer. Electroless plating bath was consist of $NiCl_2 \cdot 6H_2O$ (99.9%, Sigma Aldrich), $C_6H_5Na_3O_7 \cdot 2H_2O$ (99%, Sigma Aldrich) and $NH_3 \cdot H_2O$. $NaH_2PO_2 \cdot H_2O$ (99%, Sigma Aldrich) added as reduction agent into the solution in order to precipitate elemental Ni onto the surface of UHMWPE particles. The composition of Ni coating bath was given in Table 1.

Electroless Ni plating was realized by stirring the coating bath at 65 °C for very short duration of 5 min. The as-coated particles were filtered after coating process and then washed with distilled water. Following by washing process, composite slurry was dried at 60 °C in an oven for all day in open atmosphere. Ni content in vol% was increased by increasing the concentration of $NiCl_2 \cdot 6H_2O$ as Ni source. Furthermore, additional Ni powder (Sigma Aldrich, ~ 1 µm particle size) was mixed with Ni-coated UHMWPE powder having the highest Ni concentration.

Table 1 Composition of electroless Ni coating bath

Component	Concentration
$NiCl_2 \cdot 6H_2O$	0.19–0.38 M
$C_6H_5Na_3O_7 \cdot 2H_2O$	0.11 M
$NaH_2PO_2 \cdot H_2O$	0.83 M
$NH_3 \cdot H_2O$	13.3 vol%

M molarity

Table 2 The test materials codes

Code	vol% of Ni content	Remarks
1NP	3.98	NP: Ni coated UHMWPE
2NP	7.11	1, 2, 3: Ni source concentration in bath with increasing order
3NP	9.13	
3NP + Ni	10.88	+Ni :additive Ni powder

UHMWPE/Ni composite powders were hot pressed within a die having a diameter of 25 mm at 180 °C for 1 h. Hot pressed bulk composites with a thickness of 1.5 mm was obtained for high-efficient EMI shielding materials. The schematic illustration of electroless coating and production process were given in Fig. 1. Ni concentration in the composites were determined according to weight variation of the UHMWPE composites after Ni coating. After measuring of the weights of both coated and uncoated particles, weight ratio of the particles were converted to volume ratio and final volume content of the Ni was determined via mixing rules for the composites. Depending on the concentration of Ni source within the coating bath and additive Ni powder, samples were coded as 1NP, 2NP, 3NP and 3NP + Ni, respectively. In this nomination, "1, 2, 3" indicate Ni source concentration in the bath with an increasing order, "NP" shows Ni-coated UHMWPE and "+Ni" reflects additive Ni powder. The brief explanation of the coded samples are listed in Table 2.

UHMWPE/Ni particles were examined by SEM–EDS analysis in order to observe Ni morphology, particle size and determine the Ni purity and thickness onto the UHMWPE surfaces. XRD analysis was performed for verifying the present crystalline phases occurred during coating process. Microstructural evaluation of bulk conductive polymer composite samples were observed by SEM–EDS analysis. Hardness of composites was measured by Vickers indentation method. EMI shielding measurements were realized using transmission wave guide antenna in conjunction with network analyzer according to ASTM D4935. The EMI shielding mechanism was schematically illustrated in Fig. 2.

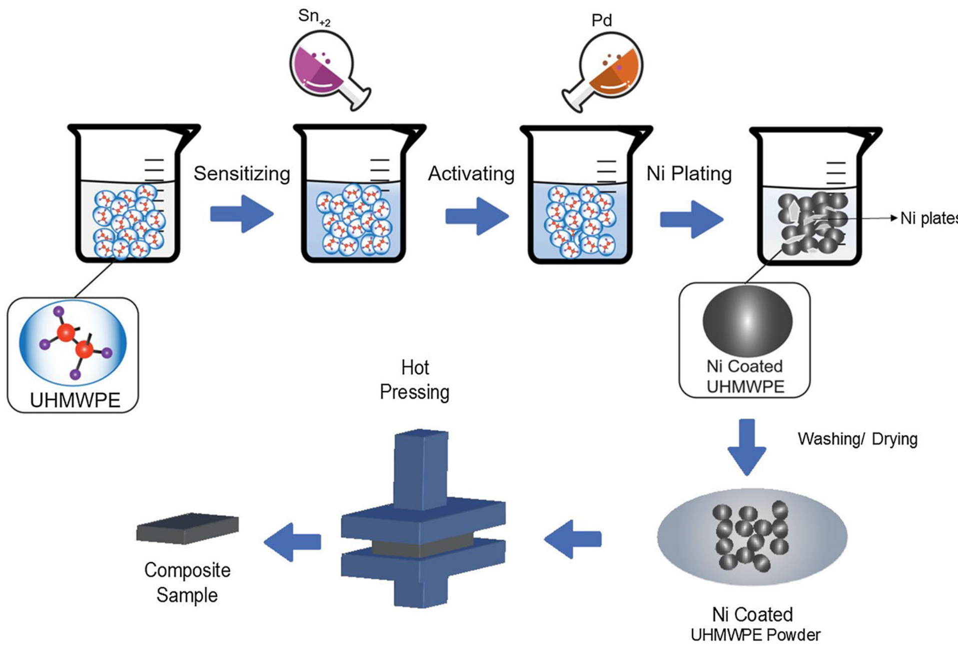

Fig. 1 The schematic illustration of electroless coating and production process

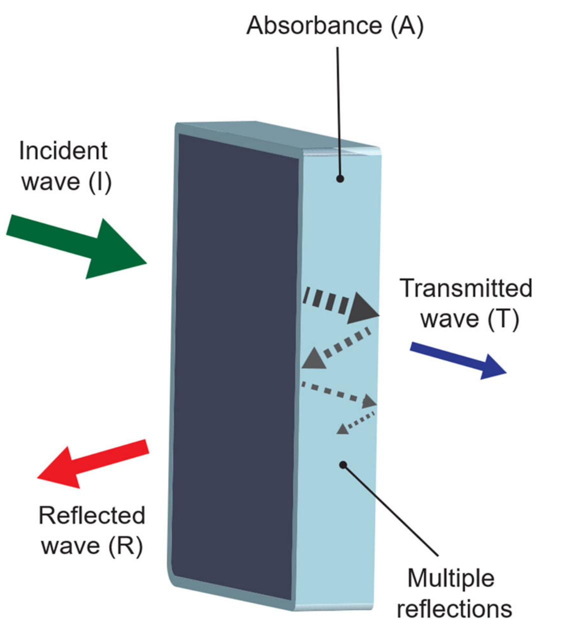

Fig. 2 Schematic representation of EMI shielding mechanism and its components

EMI SE is basically the practice of attenuating the electromagnetic wave using the proper shielding materials. Since the shielding material is a barrier between the signal source and the receiver, the shielding effectiveness is associated with the insertion loss, which indicates the attenuation magnitude [12–14]. Several test standards such as IEEE Std 299.1, MIL-STD-285, ASTM D4935 and ASTM ES7-83 have been common evaluating shielding effectiveness [15–18]. The Nicolson–Ross–Weir (NRW) method also a standard technique obtaining the permittivity and permeability of homogeneous, isotropic materials [19–22].

The total EMI shielding effectiveness is defined as the logarithmic ratio of incident power (Pi) to transmitted power (Pt) as follows [13, 23, 24]:

$$SE_{dB} = 10\log_{10}\frac{P_i}{P_t}. \tag{1}$$

Basically three contributors can be considered when a shielding material is subjected to electromagnetic wave radiation namely reflection (SE_R), absorption (SE_A) and multiple reflections (SE_M) as shown in Fig. 2. On the basis of these three phenomena, the total shielding effectiveness (SE_T) is expressed as

$$SE_T = SE_R + SE_A + SE_M. \tag{2}$$

It is obvious from the (2) that the overall shielding performance of the material is associated both absorbing and reflecting components. Reflection component is basically related to the mismatch between medium and the material interfaces. Absorption is caused by the electromagnetic wave loss and its attenuation through the material. Multiple reflections is related with secondary reflection/absorption phenomenon inside the material caused heterogeneous interfaces.

If reflecting surface is separated by a distance greater than the skin depth or absorbing component of the SE is greater than 10 dB, i.e., the EMI SE is high, SE_M term can be neglected and the overall SE can be simplified as

$$SE_T = SE_R + SE_A. \tag{3}$$

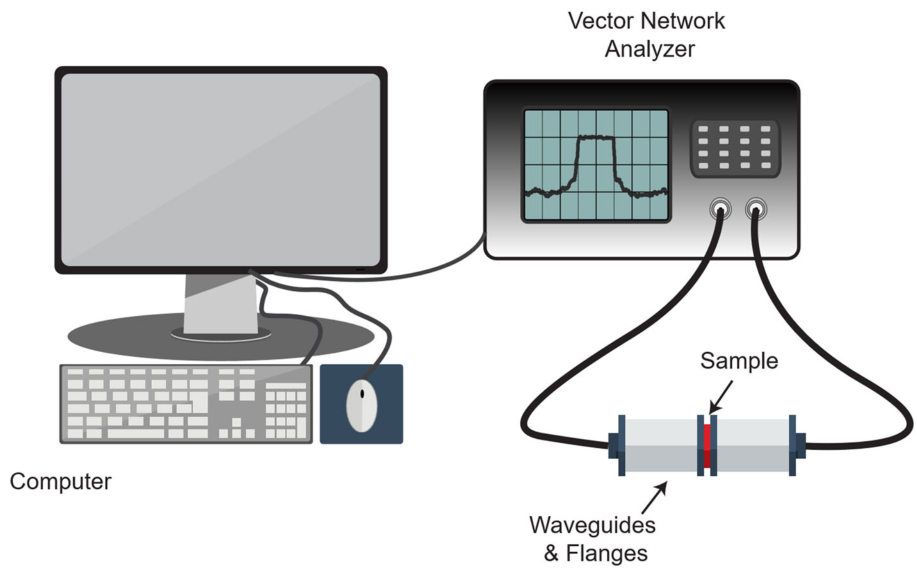

Fig. 3 Electromagnetic shielding effectiveness measurement

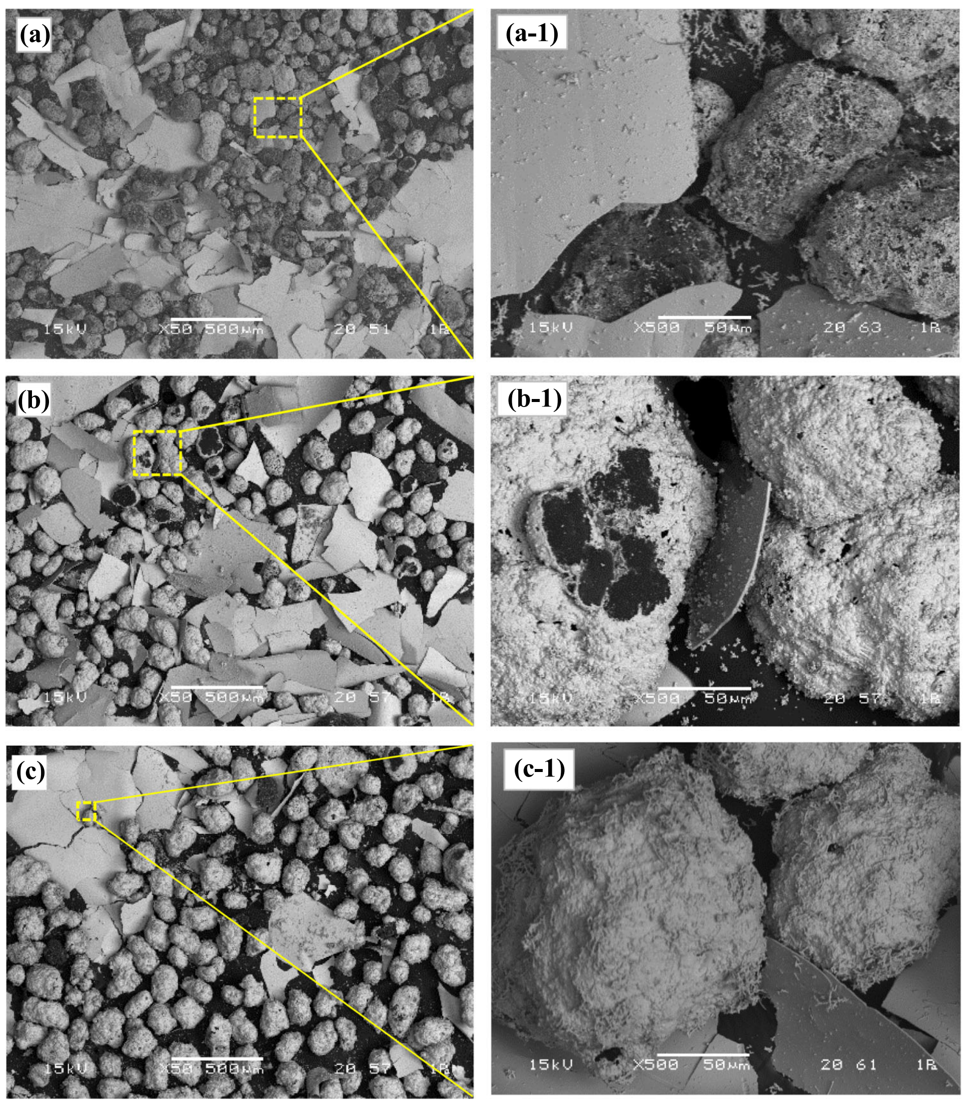

Fig. 4 SEM images of **a** 1NP, **b** 2NP and **c** 3NP powders

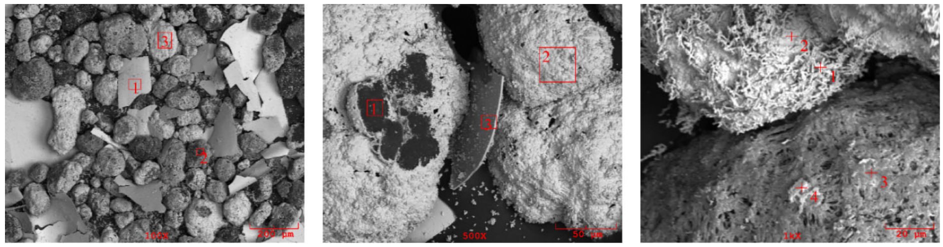

Elt.	Marks (wt.%)		
	1	2	3
C	1.274	49.966	2.251
O	-	4.888	0.816
P	9.192	4.255	6.703
Ni	**89.534**	**40.891**	**90.231**

(a)

Elt.	Marks (wt. %)		
	1	2	3
C	75.013	1.780	4.703
O	9.842	0.961	0.238
P	0.950	9.793	3.669
Ni	**14.196**	**87.466**	**91.390**

(b)

Elt.	Marks (wt. %)			
	1	2	3	4
C	3.037	0.275	26.68	4.668
O	0.203	0.010	2.435	1.971
P	0.798	0.201	3.286	7.474
Ni	**95.96**	**99.514**	**67.59**	**85.88**

(c)

Fig. 5 SEM–EDS analysis of **a** 1NP, **b** 2NP and **c** 3NP powders

Reflection and absorption components of the SE is given as

$$SE_R\ (\text{dB}) = -10\log[1 - R], \tag{4}$$

$$SE_A\ (\text{dB}) = 10\log\left[\frac{1 - R}{T}\right], \tag{5}$$

where

$$R = |S_{11}|^2, \tag{6}$$

$$T = |S_{21}|^2, \tag{7}$$

where S_{11} and S_{21} are the S-parameters and they correspond the input port reflection coefficient and the forward gain, respectively. Measurement setup which used to determine EMI SE is illustrated in Fig. 3. Scattering parameters of the prepared UHMWPE samples have been measured using a Vector Network Analyzer (Agilent ENA E5071C, 300 kHz–20 GHz). Measurements have been performed with two rectangular waveguide—flange-based test setup in the frequency range 8.2–12.4 GHz (X band) and 12.4–18 GHz (Ku band), respectively. SE_R and SE_A and then SE_T were calculated from the measured scattering parameters (S_{11} and S_{21}) considering (4)–(7) and (3).

3 Results and Discussions

Electroless Ni coating process was carried out the following reactions:

$$Pd^{2+} + Sn^{2+} \rightarrow Sn^{4+} + Pd^{0}, \tag{8}$$

$$Ni^{2+} + 2H_2\,(PO_2)^- + 2H_2O \rightarrow 2H_2\,(PO_3)^- + 2H^+ + H_2 + Ni^0, \tag{9}$$

$$Pd + Ni^{2+} \rightarrow Pd^{2+} + Ni. \tag{10}$$

According to above reactions, the mechanism for the formation of nickel coating on UHMWPE surface can be described as follows. UHMWPE powders pretreated by $SnCl_2$ solution would enhance the adsorption of Pd^{2+} ions, and then the Sn^{2+} reacted with the Pd^{2+} to form Pd catalytic nuclei on the surface of UHMWPE. The reaction can be expressed in Eq. (8). When the sensitized and activated UHMWPE powders were immersed into electroless plating bath, an autocatalytic redox reaction occurred as shown in Eq. (9). Nickel ions were reduced to metallic nickel and then aggregated together to form nickel particles. When the charged nickel particles encountered the UHMWPE surface, the Pd catalytic nuclei on the fabric possibly reacted with part of the Ni^{2+} on the nickel particles, and the reaction is represented in Eq. (10). The nickel particles were finally deposited on the surface of UHMWPE in this route [25].

SEM microstructures of Ni-coated UHMWPE powders are given in Fig. 4 with the lower and higher magnifications. It was observed that nickel particles started to accumulate on UHMWPE particles having approximately 100-µm particle size (Fig. 4a) and these particles were dispersed larger areas on surface of UHMWPE particles by increasing concentration of $NiCl_2.6H_2O$ in coating bath (Fig. 4b–c). There was almost no uncoated UHMWPE particle with increment in Ni source ($NiCl_2{\cdot}6H_2O$) concentration in the bath. As Ni concentration increased the morphology of Ni particles changed from spherical type to needle-like shape and formed Ni network between the coated particles. During electroless Ni coating, first Ni precipitates formed spherical and dense Ni thin film on the surface of UHMWPE particles (Fig. 4a, b-1). As Ni concentration increased, exceeded Ni after first Ni nucleus continued to grow on some of these spherical zone in form of needle-like stipes (Fig. 4c-1). It can be claimed that growing Ni on the first Ni nucleus occurred selectively. The color of Ni coating was turned from gray to white with increasing Ni concentration. It was found that self-precipitated white-colored Ni plates were also observed between Ni-coated powders (Fig. 4a–c). The thickness of Ni

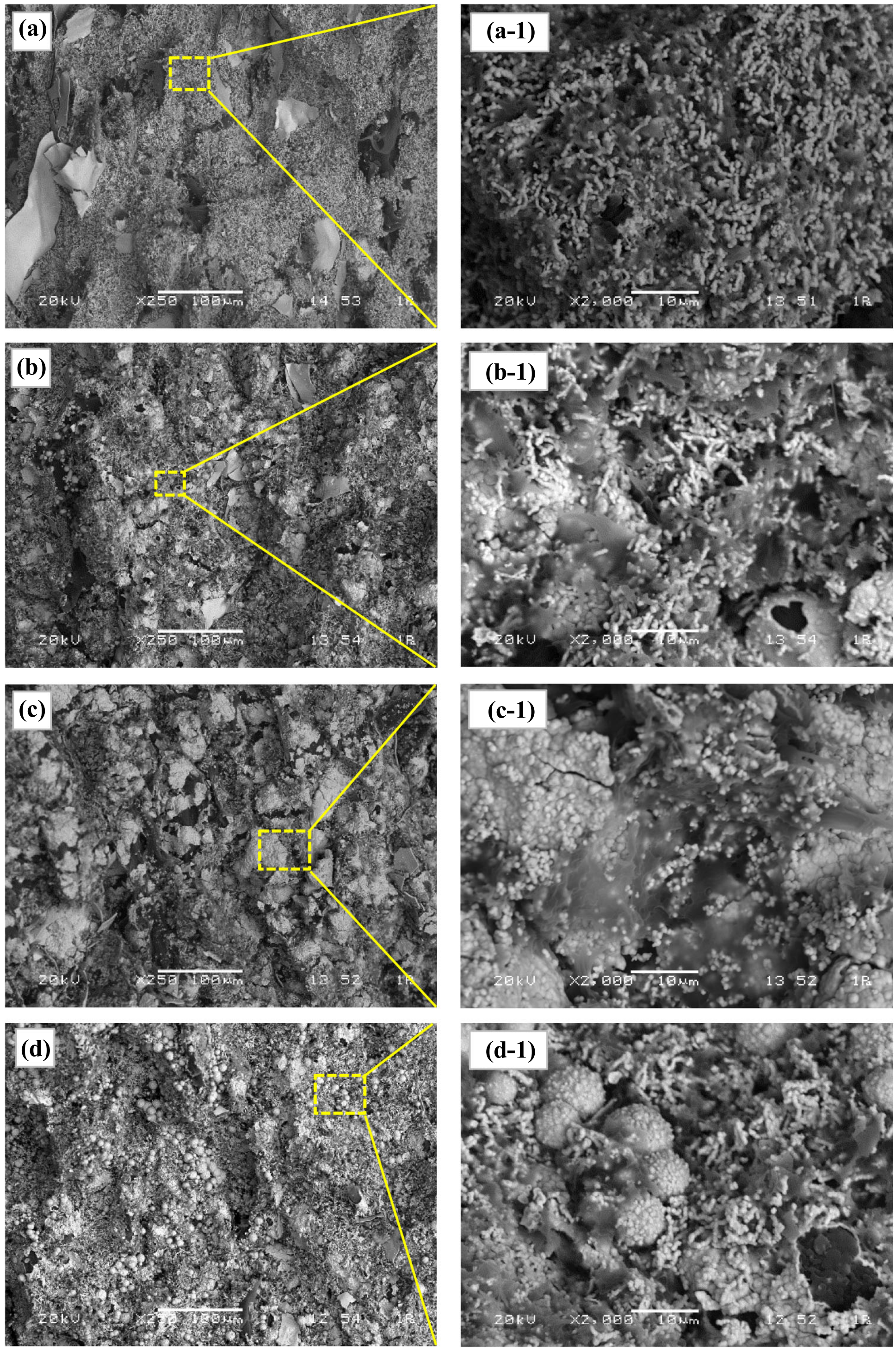

Fig. 6 Fracture surface SEM images of **a** 1NP, **b** 2NP, **c** 3NP and **d** 3NP + Ni composites

coating on surface of UHMWPE was under 2 µm (Figs. 4b-1, 6d-1) and having particle size changing from submicron to 3–4 µm (Fig. 4c-1).

SEM–EDS analysis of as-coated UHMWPE powders are given in Fig. 5. EDS analysis revealed that Ni coating on UHMWPE particles were carried out successfully and Ni content in the coating increased with increment of $NiCl_2{\cdot}6H_2O$ concentration (Fig. 5a–c). On the other hand, larger, white-colored plates belonged to metallic, self-precipitated Ni according to EDS analysis (Fig. 5a–b). The detection of some amount of P element was coming from the reduction agent ($NaH_2PO_2{\cdot}H_2O$) in the coating bath (Fig. 5).

SEM images of fracture surface of hot pressed composites are illustrated in Fig. 6. It can be expressed that

Fig. 7 SEM-dot EDS analysis of fractured surfaces of hot-molded composite samples **a** 1NP, **b** 2NP, **c** 3NP and **d** 3NP + Ni

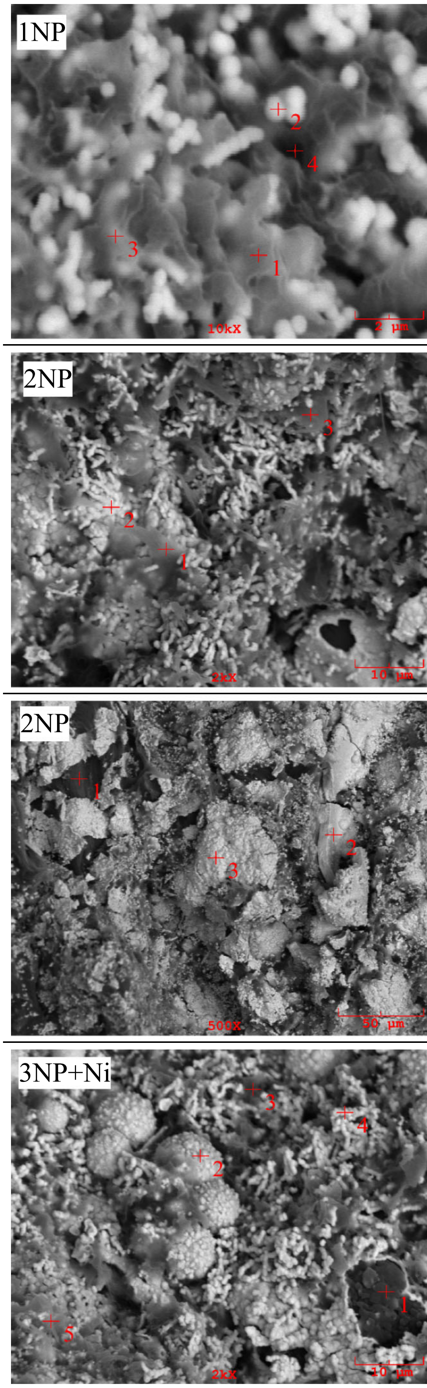

(a)

Ele.	Marks (wt.%)			
	1	2	3	4
C	47.560	26.304	46.081	32.240
O	2.961	2.982	1.491	0.894
Ni	49.479	70.714	52.428	66.866

(b)

Ele.	Marks (wt.%)		
	1	2	3
C	29.649	7.339	26.536
O	3.087	2.537	0.373
Ni	67.264	90.124	73.091

(c)

Ele.	Marks (wt.%)		
	1	2	3
C	80.838	11.162	5.890
O	12.089	1.891	0.926
Ni	7.073	86.946	93.185

(d)

Elt.	Marks (wt.%)				
	1	2	3	4	5
C	73.646	7.781	57.365	7.433	33.028
O	9.819	0.978	1.867	1.866	2.870
Ni	16.535	91.240	40.768	90.701	64.102

UHMWPE surfaces in all samples were coated with Ni as well as some self-precipitated Ni plates. Nickel concentration on the surface of the samples were increased from 1NP to 3NP samples as color of the fracture surface become brighter tone (Fig. 6a–d). Additive Ni powder was seen as light gray-colored big spheres in the SEM image of 3NP + Ni sample (Fig. 6d-1). First Ni precipitation was homogenously coated and mostly remained on UHMWPE surface without leaving after fracture of hot pressed samples. This was clearly seemed from the fully spreaded nickel films having smooth appearance on the UHMWPE grains. The Ni films become visible as the color of them become lighter and white tone with increment in Ni source concentration (Fig. 6a–d). Ni growth on that first Ni-coated zone continued as needle-like lamellae overlapping on each other and they formed some Ni network on the surface (Fig. 6b–d). This lamellar morphologhy could also be resulted from delamination of Ni particles after fracture and it can be seemed that some Ni

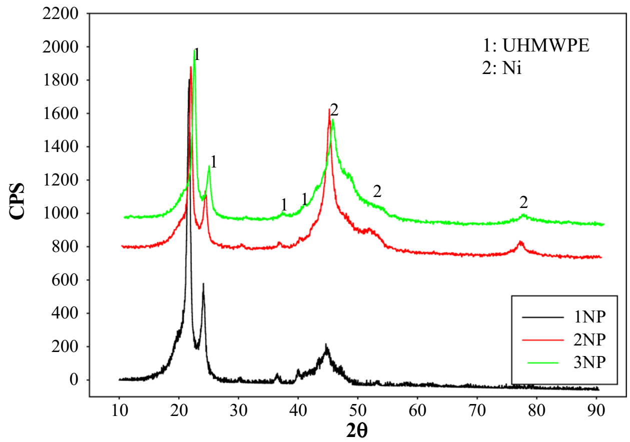

Fig. 8 XRD analysis of electroless Ni-coated UHMWPE powders

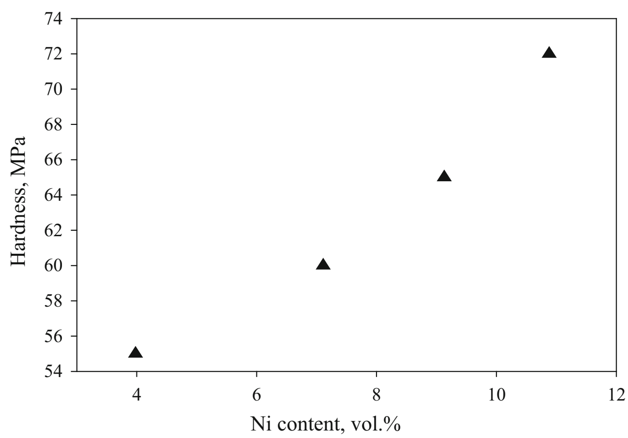

Fig. 9 Hardness variation of Ni-coated UHMWPE–Ni composites with increasing vol% of Ni content

coatings were detached from the UHMWPE grains observed as dark gray-black zone surrounded by white-coloured Ni layer (Fig. 6b-1, d-1). It can be acclaimed that some Ni precipitation was conducted from Ni coating through additive Ni spheres during hot pressing (Fig. 6d-1).

SEM–EDS analysis of bulk composites realized from fracture surface of the composites are given in Fig. 7. From the Fig. 7, it can be verified SEM microstructures (given in Fig. 6) that first Ni coating layer was homogenously taken place on the UHMWPE surface and then small spherical Ni particles were continued to precipitate on that layer (Fig. 7a) and as Ni concentration increased, Ni growing become more needle-like stipes on the surface (Fig. 7b–d). This was also confirmed by the results of dot EDS analysis taken from related points. Amounts of detected Ni element was lower in first-coated zones (Mark #1, 2 in Fig. 7a; Mark #1, 3 in Fig. 7b; Marks #3, 5 in Fig. 7d) than on white-colored Ni zones and additive Ni particles (Mark #2, 4 in Fig. 7a; Mark #2 in Fig. 7b; Marks #2, 3 in Fig. 7c; Marks #2, 4 in Fig. 7d). The detachment of some Ni layers due to fracture of the samples were understood from the EDS analysis of that surfaces detected least amount of Ni (Mark# 1 in Fig. 7c, d).

The XRD analysis was conducted to determine whether Ni coating realized or not on the UHMWPE particles using Cu-Kα radiation source with a wavelength of 1.54 nm within 10°–90° range by step-size of 0.02°. The XRD analysis revealed all of the samples was successfully Ni-coated by electroless coating method, whereas intensity of Ni element increased with increment of Ni source (from 1NP to 3NP) in the coating bath. On the other hand, peak wideness of Ni in 3NP sample was wider than that of Ni peaks in other samples which indicating the refinement of particle size of Ni precipitated on UHMWPE particles in that sample of 3NP. It can be claimed that decrement peak intensity detected in 3NP samples probably caused from increasing roughness of the Ni coating due to needle-like growing Ni stipes (Fig. 8).

Ni particles coated on UHMWPE surface act as bridge between polyethylene chains and fill in the gaps as Zhou and friends claimed in their studies [26].

Hardness values of Ni-coated UHMWPE–Ni composites are given in Fig. 9 with increasing vol% of Ni content. Hardness values of composites increased with increasing Ni content. Hardness increment is due to increasing Ni content as well as bridge formation between polymer chains by Ni

Fig. 10 Total (SET = SEA + SER) EMI shielding effectiveness results of UHMWPE samples (8.2–12.4 GHz—X band)

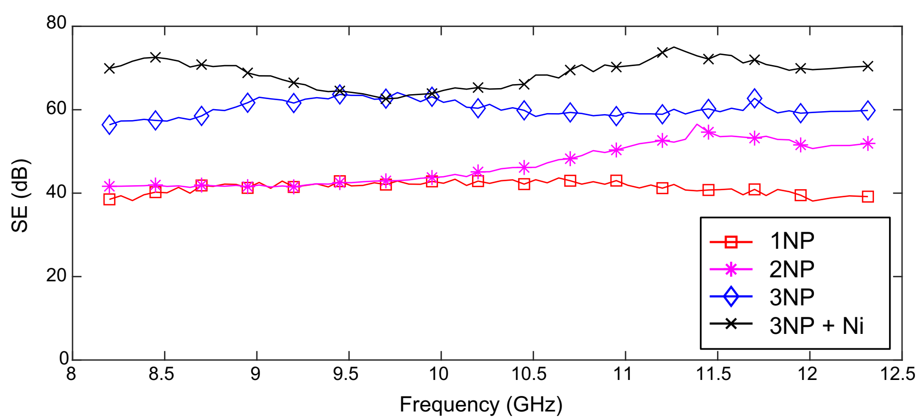

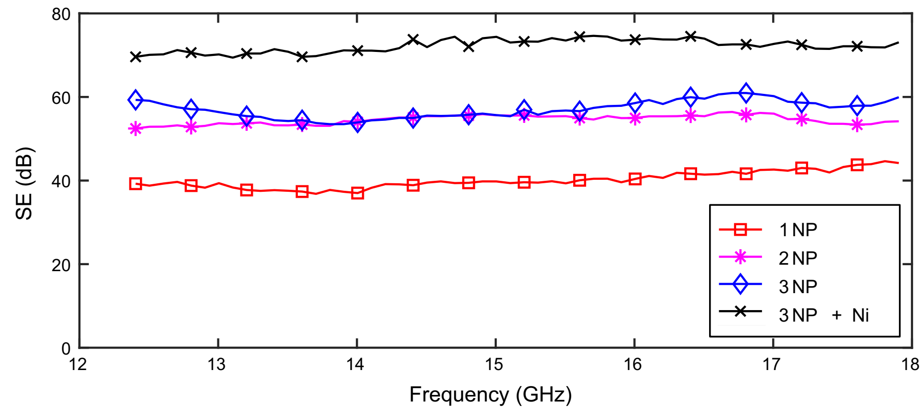

Fig. 11 Total ($SE_T = SE_A + SE_R$) EMI shielding effectiveness measurement results of UHMWPE samples (12.4–18 GHz—Ku band)

Table 3 Summary of the some literature about EMI shielding as well as our research

Reference	Polymer matrix	Filler	Preparation method	Frequency (GHz)	EMI-SE (max) (dB)
Ecco et al. [29]	Acrylonitrile–butadiene–styrene (ABS)	Carbon nanotubes and graphene nanoplatelets	Melt compounding followed by compression molding	8.2–12.4	25
Al-Saleh [28]	Ultrahigh molecular weight polyethylene (UHMWPE)	Carbon nanotubes (CNTs)	Wet mixing followed by compression molding	8.2–12.4	50
Li et al. [30]	Polydimethylsiloxane (PDMES)	Graphene/silver nanowires	Sol–gel method	8.2–12.4	34.1
Lyu et al. [31]	Polyanilines (PANI)	Aramid nanofibers (ANFs)	Composite film	8.2–12.4	30
Wen et al. [32]	Polyvinyl butyral (PVB)	Short-cut carbon fibre (SCF)	Solution casting technology	8.2–12.4	32
Ji et al. [33]	Thermoplastic polyurethane (TPU)	Carbon nanotubes	Coextrusion	8.2–12.4	60
Jiyong et al. [34]	Polytrimethylene-terephthalate (PTT) composite	Ni/polyaniline (PANi)	In situ chemical polymerization and electroless nickel plating	8.2–12.4	40
Zhou et al. [26]	PMMA	Graphene and carbon nano tube films	Bar casting method	2–18	60
Sheng et al. [35]	Ground tire rubber (GTR)	Nickel coated ultrahigh molecular weight polyethylene particles (UHMWPE@Ni)	Electroless deposition process	8.2–12.4	47.3
In our study	Ultrahigh-molecular-weight polyethylene (UHMWPE)	Ni	Electroless plating and hot pressing	8.2–18	76

particles. Bridging would probably increase the crystallinity and therefore increase the hardness of composites [27].

Total shielding effectiveness results obtained using reflection and absorption losses are shown in Figs. 10 and 11 for 8.2–12.4 GHz (X band) and 12.4–18 GHz (Ku band), respectively. Average shielding effectiveness are obtained around 40 dB, 46 dB, 59 dB and 68 dB in the 8.2–12.4 GHz range for the samples 1NP, 2NP, 3NP and 3NP + Ni, respectively. For the 12.4–20 GHz range, average results are obtained as 40 dB, 52 dB, 60 dB and 70 dB for the same samples.

It is observed that the level of electromagnetic shielding effectiveness is increased with respect to Ni concentration for both X-band and Ku-band. Even the minimum electromagnetic shielding level in all the compositions at 40 dB obtained for the 1NP composition is satisfactory for basic commercial applications. Electromagnetic shielding levels of around 70 dB is sufficient not only for commercial area but also for some applications with high-performance requirements. Composites produced in this study are fully suitable candidates especially for aerospace applications where light and high-strength materials are required.

Some results related to conducted researches about the EMI shielding as well as our research is given in Table 3. According to Table 3, our study have very promising results about metalized polymer composite shielding materials as our samples performed very high shielding within given banding range compared to most of other studied materials in Table 3, especially [28]. These reports in Table 3 were mentioned because their results about EMI shielding were remarkable through other reports mentioned in Table 3 and our study reported higher EMI shielding performance than that of these reports. One of these reports [35] were also important due to coating material and method were same with our study. In the view of Sheng's report, they conducted Ni-coated UHMWPE–GTR composites structure and their composites have very thin Ni interfaces between GTR and UHMWPE particles. Although their conductive network of composites were continuously, they obtained moderate EMI-SE levels due to voids between UHMWPE and GTR particles and vol% content of Ni was in a few degree. Al-Saleh et al. performed CNT–UHMWPE composites and their EMI-SE results were lower level compared to our samples although they used CNT which was light weight and conductive material. According to this study, their samples performed moderate EMI-SE levels compared to our samples. It can be claimed that composites reported in Al-Saleh et al. study have weak conductive network and as result of this, they obtained max 50 db of EMI-SE despite of 10 wt% CNT content. Zhou et al. obtained homogenous and thin GCF films onPMMA and result of this, their samples performed good EMI-SE which is close to that of our study.

4 Conclusions

In the present study, the following outcomes can be drawn:

(a) Metallization of UHWMPE particles by Ni was successfully realized by electroless coating method following by hot pressing route.
(b) Nickel particles started to accumulate on UHMWPE particles and were completely coated on surface of UHMWPE particles by increasing concentration of Ni source according to SEM observations of Ni-coated UHMWPE composite particles.
(c) SEM analysis of fracture surface of bulk composites revealed similar findings in that of Ni-coated particles and Ni coating has approximately 2 μm thickness.
(d) Ni particles were made some stipes from the surface of first-coated Ni layer through outer sections by growing as needle-like lamellae overlapping on each other and they formed some Ni network on the surface as confirmed SEM analysis of bulk composites.
(e) EDS analyses of both Ni-coated particles and hot pressed composites confirmed the SEM observations.
(f) XRD analysis of Ni-coated particles verified the SEM–EDS analyses and revealed that the dominant component is Ni element in the coatings as desired and some particle refinement was observed in 3NP sample.
(g) A hardness increment of 30% was obtained for Ni-coated UHMWPE–Ni composites with increasing Ni content.
(h) The level of electromagnetic shielding effectiveness is increased from 49 to 70 dB (SE_{avg}) for both X and Ku-band with respect to Ni concentration. Increasing of growth of Ni layer and formation of Ni network probably leads to higher EMI-SE ratings by forming more dense and thick Ni zones between UHMWPE particles with increment of Ni content in the composites.
i) Composites produced in this study performing 70 dB of EMI-SE are fully suitable candidates with high-performance requirements especially for aerospace applications .
(j) Our study have very promising results about metalized polymer composite shielding materials as our samples performed very high shielding within not just X band also Ku band compared to most of other reports in the open literature (Table 3).

Acknowledgements The authors would like to express their thanks to Sakarya University Electromagnetic Research Center (SEMAM) for providing its technical infrastructure during experimental studies.

Compliance with Ethical Standards

Conflict of interest Authors state no conflict of interest.

References

1. Cerezci, O.: Görülmez-Duyulmaz Risk "Elektromagnetik Alan Kirliliği." Nilufer Belediyesi (2017)
2. Mohan, R.R.; Varma, S.J.; Jayalekshmi, S.: Effective electromagnetic shield using conductive polyaniline films. Mater. Today Proc. (2019). https://doi.org/10.1016/j.matpr.2019.02.125
3. Wang, J.; Ni, M.; Wu, F.; Liu, S.; Qin, J.; Zhu, R.: Electromagnetic radiation based continuous authentication in edge computing enabled internet of things. J. Syst. Archit. (2018). https://doi.org/10.1016/J.SYSARC.2018.12.003
4. Morari, C.; Balan, I.; Pintea, J.; Chitanu, E.; Iordache, I.: Electrical conductivity and electromagnetic shielding effectiveness of silicone rubber filled with ferrite and graphite powders. Prog. Electromagn. Res. **21**, 93–104 (2011)
5. Wang, R.; Yang, H.; Wang, J.; Li, F.: The electromagnetic interference shielding of silicone rubber filled with nickel coated carbon

fiber. Polym. Test. **38**, 53–56 (2014). https://doi.org/10.1016/j.polymertesting.2014.06.008
6. Singh, A.K.; Shishkin, A.; Koppel, T.; Gupta, N.: A review of porous lightweight composite materials for electromagnetic interference shielding. Compos. Part B Eng. **149**, 188–197 (2018). https://doi.org/10.1016/j.compositesb.2018.05.027
7. Lu, L.; Xie, Y.; Teh, K.S.; Tang, Y.; Wan, Z.; Xing, D.: Highly flexible and ultra-thin Ni-plated carbon–fabric/polycarbonate film for enhanced electromagnetic interference shielding. Carbon **132**, 32–41 (2018). https://doi.org/10.1016/j.carbon.2018.02.001
8. Wang, C.; Liu, Y.; Zhao, M.; Ye, F.; Cheng, L.: Three-dimensional graphene/SiBCN composites for high-performance electromagnetic interference shielding. Ceram. Int. **44**, 22830–22839 (2018). https://doi.org/10.1016/j.ceramint.2018.09.074
9. Xu, Y.; Yang, Y.; Yan, D.-X.; Duan, H.; Zhao, G.; Liu, Y.: Flexible and conductive polyurethane composites for electromagnetic shielding and printable circuit. Chem. Eng. J. **360**, 1427–1436 (2019). https://doi.org/10.1016/j.cej.2018.10.235
10. Fujii, S.; Hamasaki, H.; Takeoka, H.; Tsuruoka, T.; Akamatsu, K.; Nakamura, Y.: Electroless nickel plating on polymer particles. J. Colloid Interface Sci. **430**, 47–55 (2014). https://doi.org/10.1016/j.jcis.2014.05.041
11. Smirnova, M.N.; Tyurenkova, V.V.; Kosinov, S.N.; Nikitin, V.F.: High-frequency electromagnetic radiation affecting moving conductive screens. Acta Astronaut. (2019). https://doi.org/10.1016/j.actaastro.2019.03.004
12. Chen, L.F.: Microwave Electronics: Measurement and Materials Characterization. Wiley, New York (2004)
13. Schelkunoff, S.A.: Electromagnetic Waves. Hardcover, New York (1943)
14. Schulz, R.B.; Plantz, V.C.; Brush, D.R.: Shielding theory and practice. IEEE Trans. Electromagn. Compat. **30**, 187–201 (1988). https://doi.org/10.1109/15.3297
15. ASTM D4935-99: Standard Test Method for Measuring the Electromagnetic Shielding Effectiveness of Planar Materials (1999). https://doi.org/10.1520/D4935-99
16. ASTM ES7-83: Test Method for Electromagnetic Shielding Effectiveness of Planar Materials. ASTM, New York (1983). https://doi.org/10.1520/ES7-83
17. IEEE Electromagnetic Compatibility Society. Standards Development Committee., Institute of Electrical and Electronics Engineers., IEEE-SA Standards Board., IEEE standard method for measuring the shielding effectiveness of enclosures and boxes having all dimensions between 0.1 and 2 m, pp 1–84. https://doi.org/10.1109/IEEESTD.2014.6712029
18. USA Department of Defense: MIL-STD-285 Military Standard Attenuation Measurements for Enclosures Electromagnetic Shielding, for Electronic Test Purposes. Washington, DC (1956)
19. Araz, İ.: The measurement of shielding effectiveness for small-in-size ferrite-based flat materials. Turk. J. Electr. Eng. Comput. Sci. **26**, 2996–3006 (2018). https://doi.org/10.3906/elk-1803-162
20. Nicolson, A.M.: Broad-band microwave transmission characteristics from a single measurement of the transient response. IEEE Trans. Instrum. Meas. **17**, 395–402 (1968). https://doi.org/10.1109/TIM.1968.4313741
21. Nicolson, A.M.; Ross, G.F.: Measurement of the intrinsic properties of materials by time-domain techniques. IEEE Trans. Instrum. Meas. **19**, 377–382 (1970). https://doi.org/10.1109/TIM.1970.4313932
22. Weir, W.B.: Automatic measurement of complex dielectric constant and permeability at microwave frequencies. Proc. IEEE **62**, 33–36 (1974). https://doi.org/10.1109/PROC.1974.9382
23. Holloway, C.L.; Hill, D.A.; Ladbury, J.; Koepke, G.; Garzia, R.: Shielding effectiveness measurements of materials using nested reverberation chambers. IEEE Trans. Electromagn. Compat. **45**, 350–356 (2003). https://doi.org/10.1109/TEMC.2003.809117
24. Wilson, P.F.; Ma, M.T.; Adams, J.W.: Techniques for measuring the electromagnetic shielding effectiveness of materials. I. Far-field source simulation. IEEE Trans. Electromagn. Compat. **30**, 239–250 (1988). https://doi.org/10.1109/15.3302
25. Liao, F.; Han, X.; Zhang, Y.; Xu, C.; Chen, H.: Carbon fabrics coated with nickel film through alkaline electroless plating technique. Mater. Lett. **205**, 165–168 (2017). https://doi.org/10.1016/j.matlet.2017.06.087
26. Zhou, E.; Xi, J.; Guo, Y.; Liu, Y.; Xu, Z.; Peng, L.; Gao, W.; Ying, J.; Chen, Z.; Gao, C.: Synergistic effect of graphene and carbon nanotube for high-performance electromagnetic interference shielding films. Carbon **133**, 316–322 (2018). https://doi.org/10.1016/J.CARBON.2018.03.023
27. Celebi Efe, G.; Altinsoy, I.; Türk, S.; Bindal, C.; Ucisik, A.H.: Effect of particle size on microstructural and mechanical properties of UHMWPE–TiO_2 composites produced by gelation and crystallization method. J. Appl. Polym. Sci. **136**, 15–18 (2019). https://doi.org/10.1002/app.47402
28. Al-Saleh, M.H.: Influence of conductive network structure on the EMI shielding and electrical percolation of carbon nanotube/polymer nanocomposites. Synth. Met. **205**, 78–84 (2015). https://doi.org/10.1016/j.synthmet.2015.03.032
29. Ecco, L.; Dul, S.; Schmitz, D.; Barra, G.; Soares, B.; Fambri, L.; Pegoretti, A.: Rapid prototyping of efficient electromagnetic interference shielding polymer composites via fused deposition modeling. Appl. Sci. **9**, 37 (2018). https://doi.org/10.3390/app9010037
30. Li, Y.; Li, C.; Zhao, S.; Cui, J.; Zhang, G.; Gao, A.; Yan, Y.: Facile fabrication of highly conductive and robust three-dimensional graphene/silver nanowires bicontinuous skeletons for electromagnetic interference shielding silicone rubber nanocomposites. Compos. Part A **119**, 101–110 (2019). https://doi.org/10.1016/j.compositesa.2019.01.025
31. Lyu, J.; Zhao, X.; Hou, X.; Zhang, Y.; Li, T.; Yan, Y.: Electromagnetic interference shielding based on a high strength polyaniline-aramid nanocomposite. Compos. Sci. Technol. **149**, 159–165 (2017). https://doi.org/10.1016/j.compscitech.2017.06.026
32. Wen, B.; Wang, X.; Zhang, Y.: Ultrathin and anisotropic polyvinyl butyral/Ni–graphite/short-cut carbon fibre film with high electromagnetic shielding performance. Compos. Sci. Technol. **169**, 127–134 (2018). https://doi.org/10.1016/j.compscitech.2018.11.013
33. Ji, X.; Chen, D.; Shen, J.; Guo, S.: Accepted manuscript flexible and flame-retarding thermoplastic polyurethane-based electromagnetic interference shielding composites. Chem. Eng. J. (2019). https://doi.org/10.1016/j.cej.2019.03.293
34. Jiyong, H.; Guohao, L.; Junhui, S.; Xudong, Y.; Xin, D.: Improving the electromagnetic shielding of nickel/polyaniline coated polytrimethylene-terephthalate knitted fabric by optimizing the electroless plating conditions. Text. Res. J. **87**, 902–912 (2017). https://doi.org/10.1177/0040517516641361
35. Sheng, A.; Yang, Y.; Ren, W.; Duan, H.; Liu, B.; Zhao, G.; Liu, Y.: Ground tire rubber composites with hybrid conductive network for efficiency electromagnetic shielding and low reflection. J. Mater. Sci. Mater. Electron. **30**, 14669–14678 (2019). https://doi.org/10.1007/s10854-019-01838-4